Available online at www.sciencedirect.com
ScienceDirect
Archives of Biochemistry and Biophysics 465 (2007) 315–319
ABB
www.elsevier.com/locate/yabbi

4′,6-Diamidino-2-phenylindole (DAPI) induces bundling of *Escherichia coli* FtsZ polymers inhibiting the GTPase activity

Esteban Nova [a,1], Felipe Montecinos [a,1], Juan E. Brunet [b], Rosalba Lagos [a], Octavio Monasterio [a,*]

[a] *Departamento de Biología, Facultad de Ciencias, Universidad de Chile, Casilla 653, Santiago, Chile*
[b] *Instituto de Química, Facultad de Ciencias Básicas y Matemáticas, Universidad Católica de Valparaíso, Casilla 4059, Valparaíso, Chile*

Received 31 January 2007, and in revised form 23 June 2007
Available online 10 July 2007

Abstract

FtsZ (Filamentous temperature sensitivity Z) cell division protein from *Escherichia coli* binds the fluorescence probe DAPI. Bundling of FtsZ was facilitated in the presence of DAPI, and the polymers in solution remained polymerized longer time than the protofilaments formed in the absence of DAPI. DAPI decreased both the maximal velocity of the GTPase activity and the Michaelis–Menten constant for GTP, indicating that behaves like an uncompetitive inhibitor of the GTPase activity favoring the GTP form of FtsZ in the polymers. The results presented in this work support a cooperative polymerization mechanism in which the binding of DAPI favors protofilament lateral interactions and the stability of the resulting polymers.

Keywords: EcFtsZ; Bundling; Polymerization; DAPI; GTPase

Escherichia coli FtsZ (EcFtsZ),[2] an essential protein for the division of the bacterial cell, is a monomeric protein of 40.3 kDa that self-assembles *in vitro* in the presence of GTP and magnesium to form protofilaments (for reviews see [1–3]). It is thought that these polymers interact to form a ring associated with the cytoplasmic membrane at the division site responsible for bacterial septation [4]. It has been established that the *in vitro* polymerization is cooperative, with a critical concentration and a lag time in the polymerization kinetics [5,6]. A nucleation mechanism with a critical concentration has been described for *Methanococcus jannaschii* FtsZ (MjFtsZ) [7], and a variation of this process involving an isodesmic assembly coupled with preferential cyclization of long polymers under crowding conditions has also been proposed [8].

FtsZ polymerization depends on the presence of magnesium and GTP [9], therefore it belongs to the guanine nucleotide binding protein family. It has intrinsic GTPase activity that is stimulated by polymerization [10,11]. FtsZ, in the presence of GDP at high protein concentrations, forms various polymer structures such as arcs and rings [12]. During polymerization, the GTPase activity is stimulated and the polymer disassembles as the GTP is spent [13]. This behavior is different from that of microtubules where tubulin-GDP remains bound to other molecules of tubulin in the body of the microtubule protected by caps of GTP-tubulin at both ends of this assembly [14]. Divalent cations [13], DEAE-dextran [15] and ruthenium red [16] induce bundling of FtsZ protofilaments inhibiting the GTPase activity.

The remarkable functional and structural similarity between tubulin and FtsZ suggest that FtsZ could be the ancestral homologue of tubulin [17] and as such, the

* Corresponding author. Fax: +56 2 276 3870.
E-mail address: monaster@uchile.cl (O. Monasterio).
[1] These authors contributed equally to this work.
[2] *Abbreviations used:* DAPI, 4′,6-diamidino-2-phenylindole; DTT, dithiothreitol; EDTA, ethylenediamidine-tetraacetic acid; GTP, guanosine 5′-triphosphate; EcFtsZ, *Escherichia coli* FtsZ; MjFtsZ, *Methanococcus jannaschhii* FtsZ; MES, 2-[*N*-Morpholino]ethanesulfonic acid; PIPES 1,4-piperazinebis ethanesulfonic acid; IPTG, isopropyl-β-D-thiogalactopyranoside.

0003-9861/$ - see front matter © 2007 Elsevier Inc. All rights reserved.
doi:10.1016/j.abb.2007.06.032

knowledge on tubulin structure can be used to predict some FtsZ structural properties. Tubulin has a high affinity binding site for the fluorescence probe DAPI that is located on the main body (tubulin S) and protected by the C-terminal region [18–20]. When bound to the tubulin heterodimer, DAPI's quantum yield increases and its fluorescence maximum shifts to the blue [19]. In this work, the binding of DAPI to EcFtsZ was characterized and its influence on the polymerization process was analyzed. EcFtsZ polymerization in the presence of DAPI showed that this fluorescence probe induced bundles of FtsZ protofilaments inhibiting the GTPase activity.

Materials and methods

Reagents

GTP (type III), DAPI, Tris, glycerol, EDTA, MES and PIPES, were purchased from Sigma Chemical Co. The HiTrap Q-Sepharose packed column was from Pharmacia. Malachite green oxalate, salts and solvents were analytical grade obtained from Merck. Ultrapure water from a Barnsted Infinity water system was used throughout.

EcFtsZ purification

The bacterial strain *E. coli* BL21 (DE3) transformed with the plasmid pMFV56 that contains the *E. coli ftsZ* gene cloned in the vector pET-28a, kindly donated by Dr. M. Vicente, was grown at 37 °C in 2 L of LB medium supplemented with 50 μg/mL kanamycin until an OD_{600nm} of 0.7 was reached in the late logarithmic phase, and expression of the protein was induced with 0.5 mM IPTG. Cells were centrifuged at 10,000*g* during 15 min at 4 °C and stored at −80 °C. Purification of the protein was achieved following the calcium-precipitation method [21]. Briefly, cells were suspended in a solution containing 50 mM PIPES, pH 6.5, 5 mM $MgCl_2$ and 1 mM EDTA and sonicated to break the cells. The protein was subjected to two cycles of calcium precipitation and suspended in the same buffer. Further purification through ion exchange chromatography (Hi-Trap Q-Sepharose column) and dialysis against 50 mM Tris–HCl, pH 8.0, 250 mM KCl and 10% glycerol was carried out. The protein was stored at −80 °C.

Protein determination

Protein concentrations were determined by measuring the absorbance at 280 nm of samples diluted 10-fold in 6 M GdmCl. A theoretical molar extinction coefficient of $11.94 \times 10^3\ M^{-1}\ cm^{-1}$ was used assuming that one mol of GDP was bound per mol of EcFtsZ [21]. Absorption spectra were obtained on a Hewlett–Packard 8452A diode array spectrophotometer.

Polymerization measurements

EcFtsZ polymerization was monitored by light scattering at 90° in a Perkin-Elmer LS-50 luminescence spectrometer setting the excitation and the emission wavelength at 430 nm to avoid DAPI interference, with bandwidths of 5 nm, using a 2% T attenuator in the emission beam filter holder to prevent overloading the photomultiplier. The polymerization was also measured through the enhancement of DAPI fluorescence under the experimental conditions described in the text. The excitation wavelength was 352 nm and the emission was fixed at 454 nm. Bandwidth of 5 nm for both excitation and emission were used and the fluorescence was recorded at 1 s intervals over the time limit indicated in Fig. 2.

EcFtsZ GTPase activity

EcFtsZ (12.5 μM) was incubated in 50 mM MES, pH 6.5, 50 mM KCl, 10 mM $MgCl_2$, in a final volume of 0.5 mL at 30 °C. The progress of the reaction was followed by taking at least three aliquots of 0.1 mL at different times and the products inorganic phosphate (Pi) and GDP were quantified. The Pi product of GTP hydrolysis was determined using the colorimetric method of malachite green [22]. In brief, the polymerization sample (70 μL) was mixed with perchloric acid to reach a final concentration of 10%. After 5 min, 50 μL of this solution were mixed in a vortex for 1 min with 800 μL malachite green reagent. One hundred microliters of citrate (34%) was added and the solution was kept on ice for 20 min before the measurement of the optical density at 630 nm. Alternatively, the concentrations of GDP and GTP were determined through chromatography of the products on a Supelcosil™ LC-18-DB or on a Mono-Q column following the OD at 260 nm in a Beckman System Gold HPLC.

Fluorescence spectroscopy

Steady state fluorescence measurements, including anisotropy, were made on a Perkin-Elmer LS-50 luminescence spectrometer, equipped with film polarizers. DAPI fluorescence intensity measurements were corrected for inner filter effects according to standard procedures [23].

Electron microscopy

Polymers were adsorbed to carbon-coated copper grids placing 10 μL of the polymerization reaction solution on the grid and negative stained with 1% uranyl acetate at room temperature. Images were taken on a Zeiss model EM-109 electron microscope at 80 kV and recorded on a KODAK TIMAX-100 film with the 35 mm camera of the microscope. Each picture was digitized directly from the film and the width of the polymers was measured using the computer program ImageJ 1.34s (http://rsb.info.nih.gov/ij/).

Data analysis

The anisotropy data were obtained as an average of 10 measurements for each experimental point. Each experiment was repeated at least twice. The experimental data were fit to the respective binding equation through the computer program Sigma Plot, Scientific Graphing Software, version 2.0, Jandel Corporation. Inhibition data were analyzed using the computer program Leonora version 1.0 for IBM PC designed by Dr. Athel Cornish-Bowden in 1992 (CNRS, CBM, B.P. 71, 31 chemin Joseph-Aiguier 13402 Marseille, France).

Results and discussion

The emission of DAPI increased approximately 4-fold upon binding to EcFtsZ and the emission maximum blue-shifted slightly from 450 to 443 nm (data not shown). DAPI (5 μM) was titrated with increasing concentrations of EcFtsZ (in the GDP form) and fluorescence anisotropy was measured (Fig. 1). The increase in anisotropy corresponds to the increase in the rotational relaxation time of DAPI upon binding to the protein. With this experiment it was not possible to reach saturation due to protein polymerization at higher concentrations. However, the additive law of anisotropy allowed the determination of the dissociation constant for one affinity binding site of DAPI ($K_d = 16.6$ μM), taking into account the 4-fold increase in quantum yield for the bound probe and assuming that the anisotropy for the bound probe was close to that for

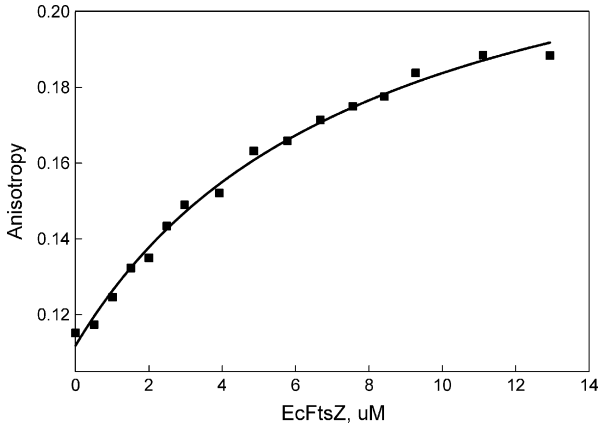

Fig. 1. Binding of DAPI to EcFtsZ followed by fluorescence anisotropy. Anisotropy of 5 μM DAPI in 50 mM MES, pH 6.5, 50 mM KCl and 10 mM $MgCl_2$ at 30 °C with increasing concentrations of EcFtsZ. The excitation wavelength was 340 nm and the bandwidth was 5 nm for both excitation and emission. The calculated value of K_d was 16.6 μM for one binding site of DAPI on EcFtsZ.

DAPI in glycerol at low temperature, i.e., 0.35, which was the case for DAPI bound to tubulin [9], and that is expected for a probe bound non-covalently with no appreciable local mobility.

The effect of DAPI on EcFtsZ polymerization was characterized following the increase in turbidity associated with the increase in light scattering. Turbidity measurements are appropriate as quantitative data after the polymers have reached a length where the turbidity is proportional to its mass. Fig. 2 shows that GTP induces a very sharp increment in the turbidity of EcFtsZ in solution at 30 °C, and after an interval the turbidity decreases reaching the initial value. In the absence of GTP, DAPI induced an increment in turbidity proportional to DAPI concentration (not shown). After GTP addition almost the same increment over the initial turbidity induced by DAPI was obtained. The kinetic behavior of the increment in turbidity induced by GTP was plotted in Fig. 2. The results show that the polymers remain in solution for a longer period as evidenced by the persistence of turbidity in the time. The critical concentration measured by light scattering is identical to that reported by Mukherjee and Lutkenhaus [13] and 5 μM DAPI slightly diminishes this value.

In order to understand the increment in stability of the EcFtsZ polymers in solution at 30 °C, the GTPase activity of EcFtsZ in the presence of DAPI was determined. EcFtsZ GTPase activity presented a typical hyperbolic kinetic behavior for the hydrolysis of GTP with a K_m of 46.4 ± 0.3 μM and a k_{cat} of $(1.3 \pm 0.3) \times 10^{-2}\ s^{-1}$. The presence of DAPI diminished both the K_m and V_{max} values. These results were plotted in Fig. 3 as both Cornish-

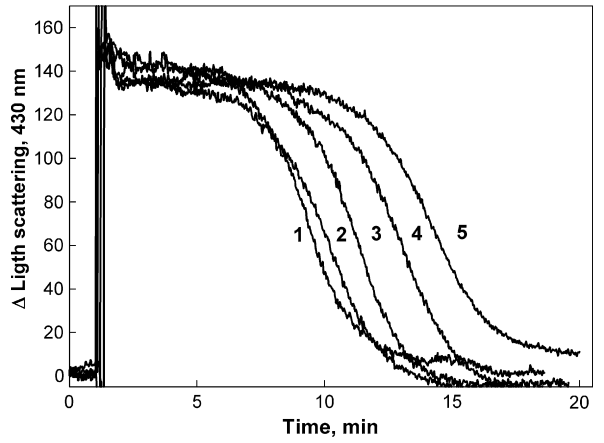

Fig. 2. Polymerization kinetics of EcFtsZ followed by light scattering in absence and presence of DAPI. EcFtsZ (12.5 μM) was polymerized at 30 °C in a solution containing 50 mM MES, pH 6.5, 50 mM KCl and 10 mM $MgCl_2$. Polymerization was started by the addition of 0.4 mM GTP. Turbidity was measured at 90° respect to the excitation beam at 430 nm. The values of light scattering before the addition of GTP increased with the addition of DAPI and in the plot were adjusted to zero. Curves 1–5 represent 0, 2.15, 3.30, 4.50 and 5.75 μM DAPI, respectively.

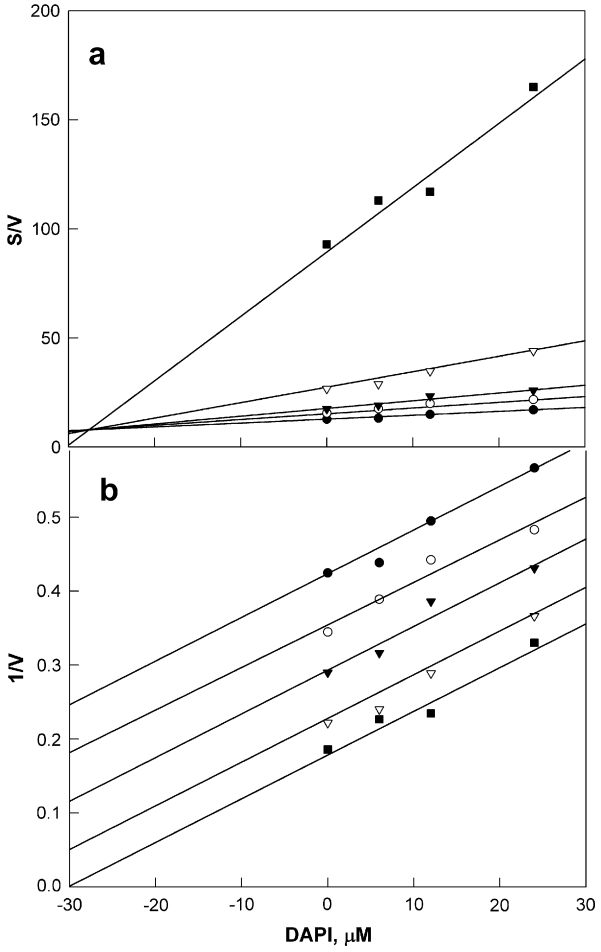

Fig. 3. Effect of DAPI on GTPase activity. The initial velocities were measured in 50 mM MES, pH 6.5, 50 mM KCl and 10 mM $MgCl_2$ at 30 °C. Protein concentration was 7.4 μM. Inorganic phosphate concentration was determined by the malachite green method. Saturation curves for GTP were transformed to represent a Cornish-Bowden plot (a) and Dixon plot (b); in both plots GTP concentrations were: 30, 45, 60, 120 and 500 μM, represented by filled circles, open circles, filled triangles, open triangles and filled squares, respectively.

Bowden (a) and Dixon (b) plots and indicate that DAPI behaves as an uncompetitive inhibitor of EcFtsZ [24], with an inhibition constant of 29.4 ± 0.3 μM, consistent with the stabilization of the polymers during the polymerization process. The same results were obtained when the GDP was quantified chromatographically as described in Materials and methods.

Electron microscopy (Fig. 4A–C) shows that DAPI induced the formation of protofilament bundles. Filaments width depended on the concentration of DAPI used, with an increment of the average width with respect to the polymers in the absence of DAPI (histograms of Fig. 4A–C). In the absence of DAPI, the polymers showed a rather homogeneous population with a majority width of 8 nm and corresponded to a double stranded filament called thick filament [7]. At 5 μM DAPI, the population became more heterogeneous with polymer widths between 8 and 400 nm in which the population of 40 nm presented the highest frequency. At 10 μM DAPI the population clearly showed a shift in

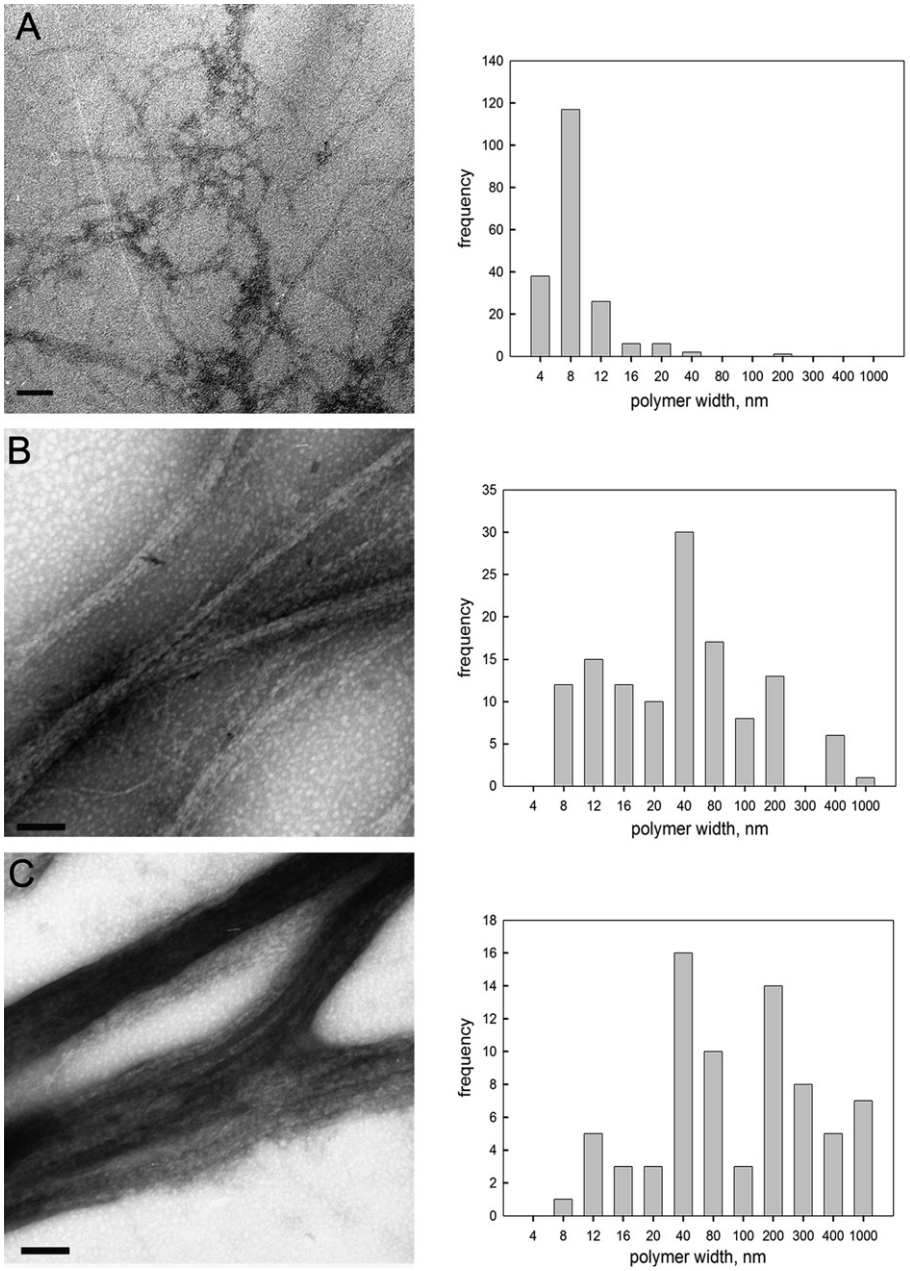

Fig. 4. Electron Microscopy of EcFtsZ polymers in absence and presence of DAPI. Electron micrographs of EcFtsZ (7.5 μM) polymers induced by GTP (0.5 mM) in the absence (A) and presence of 5 and 10 μM DAPI (B and C) at 30 °C. The polymerization solution contained 50 mM Mes pH 6.5, 50 mM KCl, 10 mM $MgCl_2$. Each mix of reaction was incubated for 20 min at 30 °C prior to GTP addition. Electron microscopy samples were taken 5 min after the addition of GTP during the lapse of polymerization. Bars: (A) 100 nm, (B) and (C) 200 nm. At the left of each figure the frequency of the distribution of the polymer width are shown in the corresponding histogram. Frequency is the number of measurements in different polymers.

the polymer width to higher values. It is interesting to point out that part of the population with a width of ~40 nm remained at 5 and 10 μM DAPI, which would correspond to the association of ~5 thick filaments [15,25]. The presence of stabilizing agents like calcium and DEAE-dextran induced the formation of polymers with 10–15 protofilaments (40–60 nm width). The common characteristic of these stabilizing agents, ruthenium red, and DAPI is the presence of positive charges, although they differ in the concentration required for the induction of sheets. Thus, calcium is in the millimolar range [26], the concentration of DEAE-dextran is sub-stoichiometric [15], while the concentrations for ruthenium red [16] and DAPI are in micromolar range (stoichiometric).

A DAPI binding site also appears in tubulin, an evolutionary related protein [3] and the binding of this probe to tubulin has not effect over microtubule polymerization [18]. DAPI binding site in tubulin is located at the interface of both subunits (α- and β-tubulin) [20]. Thus, using the knowledge of the structures of pig tubulin and MjFtsZ, a structural model of EcFtsZ has been built (E. Nova and O. Monasterio, unpublished results). The use of this model plus fluorescence resonance energy transfer experiments will help to find the location of DAPI in FtsZ, and with this information it will be possible to have a better understanding of how DAPI promotes lateral interactions.

The inhibitory effect of DAPI on the EcFtsZ GTPase activity is probably due to bundling of protofilaments, which in turn are responsible for the stability of the polymer during the polymerization process. The K_m and V_{max} of EcFtsZ GTPase activity is higher than that for tubulin, and this can be explained by the higher number of FtsZ polymers ends (short filaments) with respect to that of microtubules (long polymers with multiple subunits). In both cases the exchange of GDP by GTP and hydrolysis of the nucleotide γ-phosphate would occur principally at these ends when polymerization has reached a steady state [27,28]. Other explanation is that the exchange of nucleotide is inhibited in all protofilament subunits by the bundling induced by DAPI [29]. Free energy for the binding of DAPI to EcFtsZ at 30° C ($\Delta G^{\circ}_{binding} = -6.63$ kcal/mol, determined by anisotropy fluorescence) is a little more negative than the free energy determined from the GTPase inhibition constant ($\Delta G^{\circ}_{inhibition} = -6.28$ kcal/mol). These values suggest that the binding of one mole of DAPI per mole of EcFtsZ is responsible for the protofilament bundling and the inhibition of the GTPase activity. The uncompetitive inhibition behaviour indicates that the binding of DAPI to one site in EcFtsZ induces the bundling of the protofilaments responsible of the GTPase activity inhibition without a competitive component.

Acknowledgments

We thank the technical assistance of María Jesús Mascayano. This work was supported by Grants 1050677 and 7060162 from FONDECYT (Chile), MECESUP Grant UCH0116 and CSIC/Universidad de Chile, Grant CSIC 03/04-15.

References

[1] M. Vicente, A.I. Rico, R. Martinez-Arteaga, J. Mignorance, J. Bacteriol. 188 (2006) 19–27.
[2] J. Lutkenhaus, S.G. Addinall, Annu. Rev. Biochem. 66 (1997) 93–116.
[3] H.P. Erickson, Trends Cell Biol. 7 (1997) 362–367.
[4] E. Bi, J. Lutkenhaus, Nature 354 (1991) 161–164.
[5] L. Romberg, M. Simon, H.P. Erickson, J. Biol. Chem. 276 (2001) 11743–11753.
[6] Y. Chen, K. Bjornson, S.D. Redick, H.P. Erickson, Biophys. J. 88 (2005) 505–514.
[7] M.A. Oliva, S. Huecas, J.M. Palacios, J. Martin-Benito, J.M. Valpuesta, J.M. Andreu, J. Biol. Chem. 278 (2003) 33562–33570.
[8] J.M. Gonzalez, M. Velez, M. Jimenez, C. Alfonso, P. Schuck, J. Mingorance, M. Vicente, A.P. Minton, G. Rivas, Proc. Natl. Acad. Sci. USA 102 (2005) 1895–1900.
[9] A. Mukherjee, K. Dai, J. Lutkenhaus, Proc. Natl. Acad. Sci. USA 90 (1993) 1053–1057.
[10] A. Mukherjee, J. Lutkenhaus, J. Bacteriol. 176 (1994) 2754–2758.
[11] A. Mukherjee, J. Lutkenhaus, EMBO J. (1998) 462–469.
[12] Ch. Lu, M. Reedy, H.P. Erickson, J. Bacteriol. 182 (2000) 164–170.
[13] A. Mukherjee, J. Lutkenhaus, J. Bacteriol. 181 (1999) 823–832.
[14] H.P. Erickson, E.T. O'Brien, Annu. Rev. Biophys. Biomol. Struct. 21 (1992) 145–166.
[15] H.P. Erickson, D.W. Taylor, K.A. Taylor, D. Bramhill, Proc. Natl. Acad. Sci. USA 93 (1996) 519–523.
[16] M.K. Santra, T.K. Beuria, A. Banerjee, D. Panda, J. Biol. Chem. 279 (2004) 25959–25965.
[17] E. Nogales, K.H. Downing, L.A. Amos, J. Löwe, Nat. Struct. Biol. 5 (1998) 451–458.
[18] D. Bonne, C. Heusele, C. Simon, D. Pantaloni, J. Biol. Chem. 260 (1985) 2819–2825.
[19] M. Ortiz, R. Lagos, O. Monasterio, Arch. Biochem. Biophys. 303 (1993) 159–164.
[20] J.J. Arbildua, J.E. Brunet, D.M. Jameson, M. Lopez, E. Nova, R. Lagos, O. Monasterio, Protein Sci. 15 (2006) 410–419.
[21] G. Rivas, A. López, J. Mingorance, M.J. Ferrándiz, S. Zorrilla, A.P. Minton, M. Vicente, J.M. Andreu, J. Biol. Chem. 275 (2000) 11740–11749.
[22] P.A. Lanzetta, L.J. Alvarez, P.S. Reinach, O.A. Candia, Anal. Biochem. 100 (1979) 95–97.
[23] J. Lakowicz, Principles of Fluorescence Spectroscopy, Kluwer Academic/Plenum Publishers, New York, 1999.
[24] A. Cornish-Bowden, Fundamentals of Enzyme Kinetics, Portland Press, London, 1995.
[25] J. Lowe, L.A. Amos, EMBO J. 18 (1999) 2364–2371.
[26] X.-Ch. Yu, W. Margolin, EMBO J. 16 (1997) 5455–5463.
[27] Y. Chen, H.P. Erickson, J. Biol. Chem. 280 (2005) 22549–22554.
[28] D.-J. Scheffers, T. den Blaauwen, A.J.M. Driessen, Mol. Microbiol. 35 (2000) 1211–1219.
[29] J. Mignorance, S. Rueda, P. Gomez-Puertas, A. Valencia, M. Vicente, Mol. Microbiol. 41 (2001) 83–91.